International Journal of Solids and Structures 46 (2009) 3222–3234

Contents lists available at ScienceDirect

International Journal of Solids and Structures

journal homepage: www.elsevier.com/locate/ijsolstr

Monte Carlo simulation of complex cohesive fracture in random heterogeneous quasi-brittle materials

Z.J. Yang [a,*], X.T. Su [b], J.F. Chen [c], G.H. Liu [b]

[a] Department of Engineering, The University of Liverpool, L69 3GQ, UK
[b] College of Civil Engineering and Architecture, Zhejiang University, Hangzhou 310027, China
[c] Institute for Infrastructure and Environment, The University of Edinburgh, EH9 3JL, UK

ARTICLE INFO

Article history:
Received 26 January 2009
Received in revised form 1 April 2009
Available online 24 April 2009

Keywords:
Cohesive elements
Monte Carlo simulation
Finite element method
Random heterogeneous fracture
Quasi-brittle materials

ABSTRACT

A numerical method is developed to simulate complex two-dimensional crack propagation in quasi-brittle materials considering random heterogeneous fracture properties. Potential cracks are represented by pre-inserted cohesive elements with tension and shear softening constitutive laws modelled by spatially-varying Weibull random fields. Monte Carlo simulations of a concrete specimen under uni-axial tension were carried out with extensive investigation of the effects of important numerical algorithms and material properties on numerical efficiency and stability, crack propagation processes and load-carrying capacities. It was found that the homogeneous model led to incorrect crack patterns and load–displacement curves with strong mesh-dependence, whereas the heterogeneous model predicted realistic, complicated fracture processes and load-carrying capacity of little mesh-dependence. Increasing the variance of the tensile strength random fields with increased heterogeneity led to reduction in the mean peak load and increase in the standard deviation. The developed method provides a simple but effective tool for assessment of structural reliability and calculation of characteristic material strength for structural design.

1. Introduction

Quasi-brittle multiphase materials, such as concrete, fibre-reinforced polymer composites and toughened alloys, are widely used in engineering structures and systems in many industries. Many of them have intrinsic heterogeneous and nonlinear mechanical properties due to random distribution of multiple phases from nano-, micro-, meso- to macro-scales. Their underlying mechanical properties, dependent on their compositions, microstructures, and loading history, in turn directly determine the performance and reliability of structural systems. Therefore, a better understanding of their mechanical properties including damage and fracture by experiments and computer modelling has become one of the most critical and challenging engineering and scientific problems (Oden et al., 2003; Kassner et al., 2005). This paper is focused on finite element modelling of nonlinear fracture in these materials.

1.1. Numerical characterisation of random heterogeneity of materials

There are basically two approaches in characterising the random heterogeneity in materials numerically: the direct approach and the indirect approach. In the direct approach, the different phases in a material such as the matrix, inclusions and interfaces are explicitly modelled by finite elements and their material properties are directly assigned to the elements. The randomness in the spatial distribution of different phases is realised by randomised positions and shapes of inclusions (e.g., fibres, grains and aggregates). In the indirect approach, the material properties such as the tensile strength and the fracture energy are modelled as spatially-varying random fields with given correlation structures in the domain of interest, so different phases are implicitly modelled. To the best knowledge of the authors, there is no report available on comparing which method is superior in terms of computational efficiency and effectiveness to date.

Both the direct approach and the indirect approach have been widely employed but mostly for two-dimensional (2D) problems. As examples of the direct approach, Teng et al. (2004), Zhu et al. (2004) and Lopez et al. (2008a,b) explicitly modelled the matrix, coarse aggregates of random shapes and sizes and interfaces in concrete specimens under 2D tension and compression. Realistic and complex crack patterns were successfully simulated. Using the similar approach, Caballero et al. (2006) modelled 3D meso-scale fracture in a 80 mm concrete cube with 14 and 64 aggregates explicitly embedded in the matrix. This appears to be the only journal publication on 3D fracture of concrete using the direct approach. Trias et al. (2006) explicitly modelled fibres as plane circles in a representative volume element (RVE) of carbon fibre

* Corresponding author. Tel.: +44 151 7944897; fax: +44 151 7945218.
E-mail address: zjyang@liv.ac.uk (Z.J. Yang).

0020-7683/$ - see front matter © 2009 Elsevier Ltd. All rights reserved.
doi:10.1016/j.ijsolstr.2009.04.013

reinforced polymers. Al-Ostaz et al. (2007) carried out a similar study using Voronoi cells and Delaunay triangulation to characterise random distribution of fibres in the polymer matrix. Sfantos and Aliabadi (2007) also utilised a Voronoi tessellation method for generating artificial microstructures with randomly distributed and orientated grains to simulate the inter-granular micro-fracture evolution in polycrystalline brittle materials. No attempt has been made to obtain the statistical information of the responses using the Monte Carlo simulation (MCS) method, probably due to the high computational cost associated with generating a large number of finite element meshes and the high nonlinearity involved in the cohesive fracture process.

In the indirect approach, many new methods have been developed for generating realistic random fields of material properties (e.g., Koutsourelakis and Deodatis, 2006; Xu and Graham-Brady, 2005; Graham-Brady and Xu, 2008), but most of them have not been used in damage and fracture modelling. By modelling material properties as non-Gaussian random fields (typically Weibull distribution for concrete), Yang and Xu (2008), Bruggi et al. (2008) and Most (2005) modelled discrete crack propagation in concrete beams. All these studies used MCS to assess the structural reliability, probably thanks to the ease in generating random fields. No 3D simulation of fracture using the indirect modelling approach has been reported to the best knowledge of the authors. It is worth noting that as an indirect approach, the Weibull integral method proposed by Bazant and Planas (1998) is able to take into account the random heterogeneity of material strength but it does not require a large number of random samples. It was recently generalised to model structures with non-uniform stress fields (Bazant et al., 2007) and applied to size effect investigation (Vorechovsky and Sadílek, 2008). Although being simple and efficient, this method has limitations. For example, it can neither consider spatial correlation of local strengths nor explicitly model crack initiation and growth processes.

1.2. Numerical models for crack propagation

The continuum smeared crack models have been used to study heterogeneous and stochastic aspects of local failure since 1994 (Carmeliet and Hens, 1994; Gutierrez and De Borst, 1999; Vorechovsky, 2007). It is difficult however for existing smeared crack models to simulate macroscopic discrete cracks and particularly to calculate crack widths which are needed in serviceability design of materials and structures. It appears that more heterogeneous and stochastic models now employ the discrete crack approach, which is mostly based on the cohesive crack model (Espinosa and Zavattieri, 2003a,b; Zhou and Molinari, 2004; Tomar and Zhou, 2005; Most, 2005; Pearce and Kaczmarczyk, 2008) where cohesive interface elements are pre- or dynamically inserted into existing elemental edges. For problems with crack paths unknown a priori, fine meshes are needed to minimise the dependence of crack paths on the initial FE mesh. This often leads to large-scale nonlinear equation systems, of which the computational costs often become prohibitively expensive when uncertainties are further taken into account by using MCS method or non-MCS stochastic methods. To overcome this difficulty, Yang and Xu (2008) developed a heterogeneous cohesive rack model based on Weibull random fields of fracture properties and remeshing with a new crack growth direction criterion. The model was able to predict more realistic tortuous crack paths and assess the structural reliability using the MCS. Compared with models with pre-inserted cohesive interface elements (CIEs), this remeshing-based model has much higher computational efficiency as it employs relatively coarse meshes with far fewer nonlinear CIEs without compromising the accuracy. However, this model becomes cumbersome when modelling complex crack patterns. Other non-classical models, such as lattice model (Blair and Cook, 1998; Cusatis et al., 2003a,b) have also been developed in fracture modelling of heterogeneous materials.

Clearly only 2D fracture has been modelled in the limited existing studies which considered heterogeneity and randomness. Statistical analysis using MCS has been rarely conducted due to its high computational cost. The mesh-objectivity of results in stochastic fracture modelling remains a challenging problem in all crack models, due to unresolved puzzles on crack resolution or fractals (Carpinteri et al., 2006).

1.3. Methods of extracting statistical responses

To date, the most general and robust method for processing and estimating the uncertainty or reliability of structural performances is still the Monte Carlo simulation method. Compared to other methods such as stochastic finite element method which requires the variability of random parameters be small (Altus and Givli, 2004), the MCS method is applicable to any problems for which the deterministic problem can be solved, as long as the sample number is sufficiently large. For random heterogeneous multiphase materials involving high nonlinearity and fracture, the MCS method seems the best option. In fact, all the very limited 2D studies with statistical analysis used this method (Most, 2005; Vorechovsky, 2007; Yang and Xu, 2008; Bruggi et al., 2008). It may be noted that a 3D study (Papadrakakis et al., 2008) treats concrete as a homogeneous materials although the MCS method is used to generate response statistics from simulations with different material properties.

The biggest disadvantage of the MCS is that it requires a considerable number of samples from the same number of nonlinear analysis. Nonlinear modelling of multiple crack propagation in multiphase materials is very time consuming, even for small specimens as RVEs. This makes supercomputers a necessity when it is used if a large number of random variables are considered. To overcome the bottleneck of computation cost, a variety of exciting new techniques are emerging to reduce the required sample number (e.g., Webster, 2007; Ganapathysubramanian and Zabaras, 2007; Au and Beck, 2001). However, none of these new techniques has been applied to fracture modelling of complex multiphase materials.

1.4. Scope of this study

This study develops a numerical method to simulate the complex 2D fracture process in quasi-brittle materials considering random heterogeneous fracture properties, in a view to critically assess their performance and structural reliability under external loadings. In this method, all the finite elemental edges in the domain of interest are regarded as potential cracks, modelled by pre-inserted cohesive interface elements with tension and shear softening laws. The special features of this study are: (i) the cracks are modelled by a special type of "cohesive elements" (COH2D4) in the general-purposed finite element analysis package ABAQUS (2007). The cohesive elements, only available in Abaqus Version 6.5 or higher, are designed to model bonded interfaces. Their effectiveness in modelling cracks has hardly been validated. Another intention of this study is to fully exploit the powerful pre/post-processing modules and standard/explicit solvers of Abaqus in modelling complex fracture problems; (ii) the softening laws of the cohesive elements are modelled as spatially-varying Weibull random fields, i.e., an indirect approach is used to model the random heterogeneity of fracture properties; (iii) the statistical information of structural responses is obtained by extensive Monte Carlo simulations for a range of heterogeneity levels, which have rarely been conducted before; (iv) a concrete specimen under uniaxial tension is modelled as a benchmark problem with extensive parametric studies and investigation of the effectiveness and efficiency of rel-

evant numerical algorithms; and (v) the method is simple to implement and is potentially very powerful for modelling stochastic fracture problems under various loading conditions.

2. The methodology

2.1. Modelling procedure

The proposed method involves the following procedure:

(1) meshing the domain using Abaqus/CAE and generate an input file. Because the simulated crack patterns are dependent upon the initial mesh, triangular elements are preferred in the domain of interest so that curved crack paths can be modelled with good accuracy;
(2) inserting cohesive elements into the initial mesh. This is done using a small in-house computer program. Fig. 1a illustrates a typical node connected with eight triangular elements in the initial mesh. This node is first replaced by eight separate nodes at the same position, and eight cohesive elements are then generated along the element edges around it (Fig. 1b). Fig. 1c illustrates the 2D four-noded cohesive element with zero in-plane thickness (which is exaggerated for clarity);
(3) generating a random sample of fracture properties in the domain of interest;
(4) assigning the fracture properties to all the cohesive elements and generate an input file for Abaqus. In the random sample, the fracture properties are only calculated at the grid points, and the random sample grid normally does not coincide with the finite element mesh. In this study, the fracture properties of a cohesive element are assigned with those at the grid point closest to its centre;
(5) solving the problem using Abaqus standard/explicit solvers; and
(6) repeating steps (3–5) for a sufficient number of random samples, as required by the MCS method, and conduct statistical analysis.

This procedure can be automated by running a batch file.

2.2. Cohesive elements with damage in Abaqus

The cohesive crack model proposed by Barenblatt (1959) and Dugdale (1960) and the fictitious crack model by Hillerborg et al. (1976) enable the simulation of the energy dissipation process in the fracture process zone (FPZ) during fracture. They assume that there exist a normal traction t_n and a tangential traction (shear cohesion) t_s across the crack surfaces, through mechanisms such as material bonding, aggregate interlocking and surface friction in the FPZ. The tractions decrease monotonically as functions of the corresponding relative displacements of the crack surfaces (crack opening displacement δ_n and crack sliding displacement δ_s in 2D problems), which is often termed tension or strain softening. Typical linear softening curves for t_n–δ_n and t_s–δ_s are illustrated in Fig. 2a and b, respectively, where δ_{nf} and δ_{sf} are the critical relative displacements when the tractions diminish. A linear ascending branch is added in each softening curve to model the initially

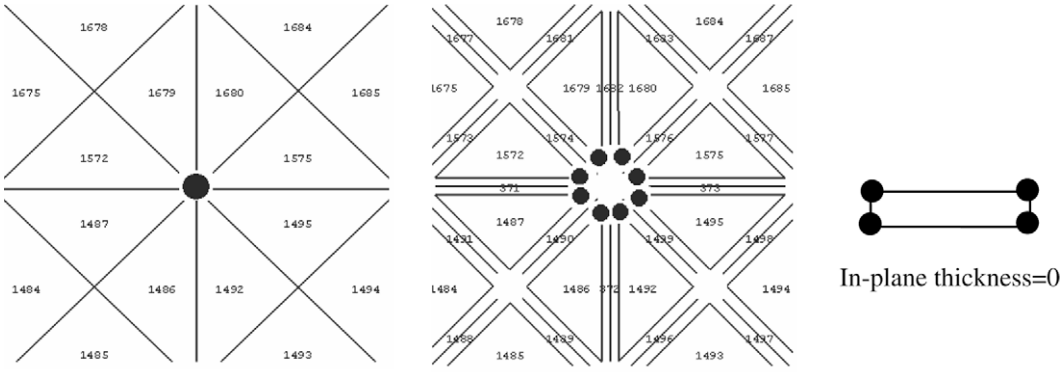

Fig. 1. Inserting cohesive elements in the initial mesh.

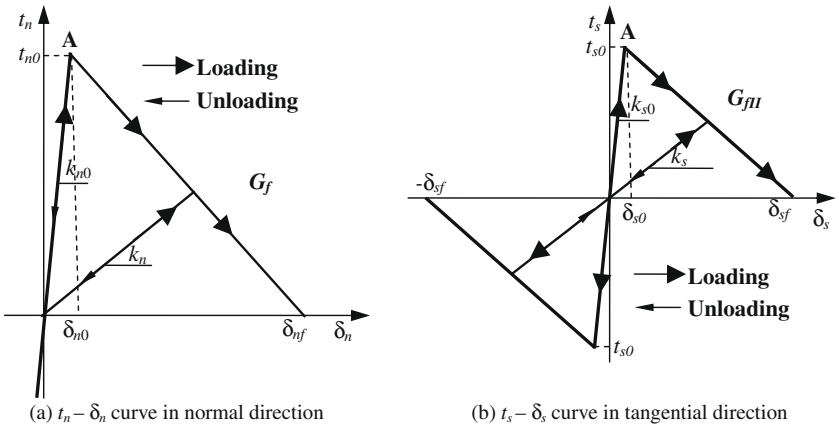

Fig. 2. Linear softening laws for the cohesive element.

un-cracked material. The unloading paths are also indicated. The areas under the curves in Fig. 2a and b represent, respectively, the mode-I fracture energy G_f and twice the mode-II fracture energy G_{fII}. Both G_f and G_{fII} are treated as material properties in this study. The initial tensile stiffness k_{n0} before the tensile strength t_{n0} is reached should be high enough to represent the un-cracked material, but not too high to cause numerical ill-conditioning. A reasonable initial shear stiffness k_{s0} is also needed before the shear strength t_{s0} is reached. k_{n0} and k_{s0} can be determined by a trial and error approach. If δ_n is negative during loading increments or iterations, a compressive stiffness of magnitude equal to k_{n0} is assigned in order to prevent penetration of crack surfaces.

The cohesive element COH2D4 with zero in-plane thickness in Abaqus is based on the cohesive crack model, and its constitutive behaviour can be described by the softening laws similar to Fig. 2. The resilient feature of COH2D4 is that its formulation is based on the damage mechanics framework, within which the stiffness k_s and k_n upon unloading and reloading are degraded as δ_s and δ_n increase, due to irreversibly progressive damage. The damage is characterised by a scalar index D representing the overall damage of the crack caused by all physical mechanisms. It is a function of the so-called effective relative displacements δ_m combining the effects of δ_s and δ_n:

$$\delta_m = \sqrt{< \delta_n >^2 + \delta_s^2} \tag{1}$$

where < > is the Macaulay bracket and

$$< \delta_n >= \begin{cases} \delta_n, & \delta_n \geqslant 0 \text{ (tension)} \\ 0, & \delta_n < 0 \text{ (compression)} \end{cases} \tag{2}$$

For the linear softening law in Fig. 2, the damage evolves according to

$$D = \frac{\delta_{mf}(\delta_{m,\max} - \delta_{m0})}{\delta_{m,\max}(\delta_{mf} - \delta_{m0})} \tag{3}$$

where $\delta_{m,max}$ is the maximum effective relative displacement attained during the loading history. δ_{m0} and δ_{mf} are effective relative displacements corresponding to δ_{n0} and δ_{s0}, and δ_{nf} and δ_{sf} in Fig. 2, respectively. Exponential softening law is also available in Abaqus. Eq. (3) indicates that D monotonically evolves from 0 to 1 upon further loading after the initiation of damage.

The stiffness k_n and k_s can then be calculated as

$$k_n = (1 - D)k_{n0} \tag{4a}$$

$$k_s = (1 - D)k_{s0} \tag{4b}$$

The tractions are affected by the damage according to

$$t_n = \begin{cases} (1 - D)\bar{t}_n, & \bar{t}_n \geqslant 0 \\ \bar{t}_n, & \bar{t}_n < 0 \text{ (no damage to compressive stiffness)} \end{cases} \tag{5}$$

$$t_s = (1 - D)\bar{t}_s \tag{6}$$

where $\bar{t}_n$ and $\bar{t}_s$ are the traction components predicted by the elastic traction-separation behaviour for the current separation without damage.

Apart from the damage evolution law given by Eq. (3), a damage initiation law referring to the beginning of stiffness degradation is also needed. This study assumes a quadratic nominal stress law, i.e., the damage is assumed to initiate when a quadratic interaction function involving the nominal stress ratios reaches a value of one:

$$\left\{\frac{\langle t_n \rangle}{t_n^0}\right\}^2 + \left\{\frac{t_s}{t_s^0}\right\}^2 = 1 \tag{7}$$

The classical homogeneous materials based cohesive model assumes that the softening laws as shown in Fig. 2 apply uniformly to the whole material domain. This assumption neglects the intrinsic heterogeneity in the tensile strength and fracture energy, and takes a "fracture homogenization" approach. In other words, both tensile strength and fracture energy, determined from direct tension tests or bending beam tests, are averaged values over a finite area of surface for ease of engineering use. The conventional definitions of fracture properties can be generalised by considering heterogeneity randomly distributed in space, i.e.

$$R = R(\mathbf{x}, \omega) \tag{8}$$

where $\mathbf{x}$ denotes the Cartesian coordinate vector of any point in the domain, ω a random sample and R one of the fracture properties, such as the strength t_{n0} and t_{s0}, the fracture energy G_f and G_{fII}, or more generally, the two cohesive laws shown in Fig. 2.

The bulk material properties such as Young's modulus and Poisson's ratio can also be treated in the same way but they are assumed to be constants for simplicity so that this study can be focused on the effects of spatially random distributed fracture properties.

2.3. Fracture properties characterised as Weibull random fields

Assuming that the material strength follows the Weibull distribution (e.g., Bazant et al., 2007), the probability of a material of size V with strength less than y is

$$P(y) = 1 - \exp\left[\frac{V}{V_0}\left(-\frac{y}{s_0}\right)^m\right] \tag{9}$$

where s_0 and m are scale and shape parameters, respectively. V_0 is the volume of RVE. Once V and V_0 are known in a fracture model, the variance and mean of the Weibull distribution can be determined by choosing appropriate values for the parameters s_0 and m, or vice versa.

Let $X(\mathbf{x}, \omega)$ be a stationary Gaussian random field with zero mean and unit variance, which can be obtained using the spectral representation method (Xu, 2005). The corresponding translated random Weibull field $Y(\mathbf{x}, \omega)$ can be obtained through the point-wise monotonic nonlinearity as

$$Y(\mathbf{x}, \omega) = P^{-1}(\Phi(X(\mathbf{x}, \omega))) \tag{10}$$

where $\Phi(.)$ is the standard normal cumulative density function.

The correlation function of 2D Gaussian random field $X(\mathbf{x}, \omega)$ is chosen as

$$\rho(\mathbf{x}_1 - \mathbf{x}_2) = \exp\left[-\frac{\pi|\mathbf{x}_1 - \mathbf{x}_2|^2}{l_c^2}\right] \tag{11}$$

where l_c is the correlation length. Since l_c is numerically close to the correlation length of $Y(\mathbf{x}, \omega)$, it can be used to indicate the characteristic length of a heterogeneous medium, e.g., the average aggregate size in concrete. It should be noted that mapping Gaussian random fields to Weibull ones using Eq. (10) may lead to correlation distortion, particularly for highly skewed distributions. This problem is effectively tackled in this study using an empirical iterative method (Xu, 2005).

3. A numerical example

A concrete specimen under uniaxial tension was modelled using the developed method as an example. The geometry, boundary conditions and bulk material properties are illustrated in Fig. 3. Note that Lopez et al. (2008a) simulated the same specimen using the direct modelling approach but no MSC was carried out.

3.1. Finite element modelling

The elastic bulk of concrete was modelled using 4-noded isoparametric and 3-noded constant strain plane stress elements.

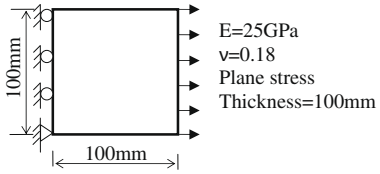

Fig. 3. A concrete specimen under uniaxial tension.

The cracks were modelled using the 4-noded cohesive elements. To investigate the mesh dependence of crack patterns and load–displacement curves, two initial meshes were modelled as shown in Fig. 4. The coarse mesh (Fig. 4a) has 2104 nodes and 1000 cohesive elements, and the fine mesh (Fig. 4b) has 8936 nodes and 4000 cohesive elements. In order to minimise the boundary effects on the crack initiation and propagation, no cohesive elements were inserted in the two narrow strips adjacent to the constraints on the left and the applied forces on the right.

The concrete tensile strength t_{n0} was modelled by random fields, namely, $t_{n0} = t_{n0}(\mathbf{x}, \omega)$ and the mode-I fracture energy $G_f = 0.15\text{N/mm}$ was assumed constant. This implied that the failure crack opening displacement $\delta_{nf} = 2G_f/t_{n0}(\mathbf{x}, \omega)$ was also a random field. The tensile strength was assumed to have a mean value of 3.5 MPa. Due to the lack of experimental data, the shear fracture properties were simply assumed to be the same as the normal ones: $t_{s0} = t_{n0}(\mathbf{x}, \omega)$ and $G_{fII} = G_f = 0.15\text{N/mm}$, indicating that the normal fracture properties were completely correlated to the shear ones. The fracture energies and more generally, the softening laws (Fig. 2) could also be modelled as random fields with ease, as in a previous study based on remeshing (Yang and Xu, 2008).

For one Monte Carlo simulation, 500 Weibull random samples of tensile strength were generated and mapped to the coarse mesh. The Weibull random samples with a 32×32 grid were generated by Eqs. (9)–(11), leading to a resolution of 3.125 mm per grid spacing. Three correlation lengths $l_c = 6.25$, 12.5 and 25 mm were modelled. They are within the range of aggregate sizes (10–40 mm) normally used in concrete. Three values of variance for t_{n0} and t_{s0}, $Var = 0.1, 1.0$ and $1.5\ \text{MPa}^2$, were modelled. In total, nine MCS were carried out with 4500 random samples generated and the same number of nonlinear analyses conducted for the coarse mesh. A few analyses were also conducted for the fine mesh. To demonstrate the importance of modelling material heterogeneity, homogeneous simulations with $t_{n0} = t_{s0} = 3.5$ MPa and $G_{fII} = G_f = 0.15\text{N/mm}$ throughout the domain were also undertaken.

The specimen was subjected to a uniformly distributed displacement at the right surface of the specimen, i.e., a displacement-controlled loading scheme was used. This assumes fixed platens against rotation are used at the right and left boundaries of the specimen. If rotation of the loading platens is allowed, the structural responses may be different (van Mier, 1996; Vorechovsky, 2007). All analyses were ended at a displacement $d = 0.3$ mm. Both Abaqus/standard and Abaqus/explicit were tried to solve the nonlinear equation systems. The concrete was assigned a density of $2.5 \times 10^3\ \text{kg/m}^3$ in the explicit quasi-static analyses. An initial stiffness in the softening laws $k_{n0} = k_{s0} = 25000\ \text{MPa/mm}$ was used for all the simulations after trial and error.

A computer with an Intel Xeon CPU@3.16 GHz was used for all the analyses.

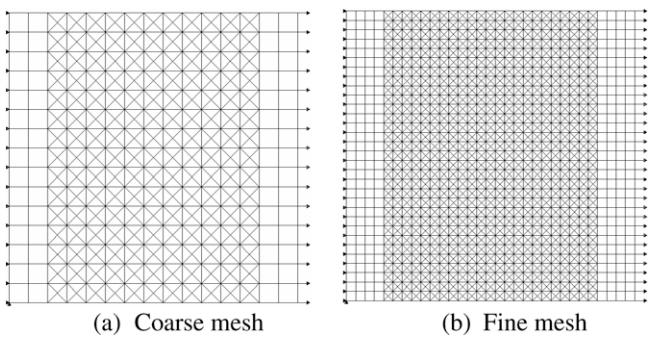

Fig. 4. Initial finite element meshes.

3.2. Significance of modelling material heterogeneity

The final crack patterns from the homogeneous simulations are shown in Fig. 5a and b for the coarse and fine meshes, respectively. For each mesh, all the vertical cohesive elements opened at the same rate during the fracture process, leading to uniformly distributed cracks of the same width. This is expected because the maximum tensile stress is horizontal everywhere under the uniaxial loading. The maximum shear stress is on the 45° plane and it is only half of the maximum tensile stress, and thus no diagonal shear cracks appeared. Clearly this failure mode is unrealistic and has never been observed in experiments. The crack pattern is clearly mesh-dependent, i.e., more vertical cracks will inevitably be predicted with finer meshes.

Fig. 6 illustrates the fracture process modelled using the coarse mesh and a typical Weibull random sample (RF1) of tensile strength with $Var = 0.1\ \text{MPa}^2$ and $l_c = 12.5$ mm. The random sample (Fig. 6a) is described by the filled contours, with deep blue areas indicating low tensile strength (e.g., defects, voids, weak inclusions etc.), and dark red[1] areas representing high tensile strength (e.g., strong aggregates). When the displacement is small (Fig. 6b), a number of small visible cracks, displayed by the opened cohesive elements in red (the red colour represents high damage index D($D = 1$ means complete failure)), initiate in the blue areas at the boundary and inside the domain. Closer examination of the deformed mesh shows that more cohesive elements have experienced damage but are invisible because their damage index D is small. As the displacement increases, the visible cracks continue to widen. A few vertical cracks are then linked by diagonal cracks and merged into major cracks, while the other cracks are closed due to stress redistribution (Fig. 6c). The specimen fails by a major crack passing through the weakest area (Fig. 6d).

As examples, a few more crack patterns from heterogeneous modelling are shown in Fig. 7 together with the corresponding random samples with $Var = 0.1\ \text{MPa}^2$ and $l_c = 12.5$ mm. It is reasonable to expect that any two specimens under the same test condition will hardly fail with the same crack patterns, and it is virtually impossible to directly validate the predictions of the final crack patterns. Nevertheless, the predictions from heterogeneous modelling look far more realistic than those from homogeneous modelling (Fig. 5). Figs. 6 and 7 also demonstrate the flexibility and power of the developed numerical method for simulating a variety of failure modes.

3.3. Mesh dependence of results

The random sample RF1 in Fig. 6a was also mapped to the fine mesh and the fracture process predicted is shown in Fig. 8. A good similarity can be seen between Figs. 6b–d and 8a–c, especially when the displacement is small. The discrepancy increases as the post-peak displacement increases, indicating that some mesh-

[1] (For interpretation of color mentioned in this figure, the reader is referred to the web version of the article.)

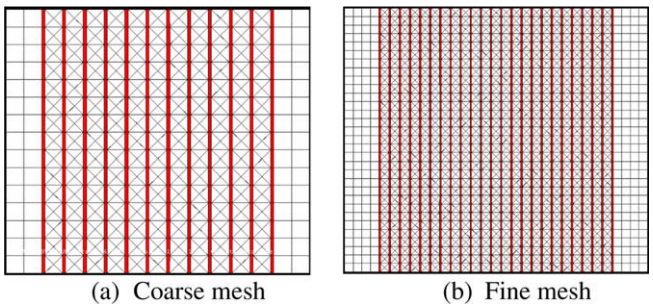

Fig. 5. Crack patterns predicted using the homogeneous model (displacement $d = 0.3$ mm).

dependence is still evident. However, this problem is much less serious than that in the homogeneous simulations (Fig. 5). As will be discussed in Section 3.5, the mesh-dependence problem diminishes gradually as the variance increases.

Fig. 9 compares the predicted average stress–displacement curves using the four random samples in Figs. 6 and 7. The average stress was found from the total reaction force in the constraints divided by the cross-sectional area of the specimen. It is clear that the curves from homogeneous model are incorrect and sensitive to the mesh density, whereas those from heterogeneous model, showing stochasticity in the post-peak branch, are close to the typical experimental curve (Hordijk, 1992) with far less mesh-sensitivity. The peak stresses from the coarse mesh and the fine mesh using RF1 are virtually the same (3.19 and 3.14 MPa, respectively).

3.4. Effects of variance on crack patterns and mesh-dependence

Physically, a higher variance in the tensile strength may be caused by poor compaction, inclusion of very weak or strong aggregates, variable adhesion between the cement paste and aggregates, and existence of voids. Numerically, a higher variance means a larger difference between the maximum and minimum values in the random sample. Figs. 10a and 11a show two random samples using the same underlying Gaussian field as RF1 but with $Var = 0.5$ MPa^2 and $Var = 1.5$ MPa^2, respectively. The fracture processes are illustrated in Figs. 10b–d and 11b–d, respectively. It is clear that although the cracks initiate at the same areas with the lowest tensile strength, the final crack patterns are very different. As the variance increases, the vertical cracks are easier and earlier to be linked by the diagonal cracks and merged into a major crack. This is because when the variance is small, the tensile strength values in the cohesive elements are little different so that more cohesive elements in larger areas are mobilised to resist fracture, making the crack patterns more complicated. As the variance increases, the weaker areas become even weaker and the fracture paths or the "weakest link" can be more easily found, as fewer weak cohesive elements contribute to fracture resistance.

The fine mesh was also modelled using the same random sample with $Var = 1.5$ MPa^2 as in Fig. 11a. The predicted fracture process (Fig. 12a–c) is very close to that from the coarse mesh (Fig. 11b–d). The load–displacement curves are virtually the same. This indicates that as the variance increases, the mesh-dependence problem becomes a less serious issue. This is because as the variance becomes larger, the "weakest link" becomes less sensitive to the mesh density and the crack path is much easier to be found in numerical modelling.

3.5. Numerical solution algorithms

All the aforementioned simulations were carried out using Abaqus/Standard as static stress analyses. To tackle possible numerical instability due to material softening in the cohesive elements, an option "Stabilize" was used with the default dissipated energy

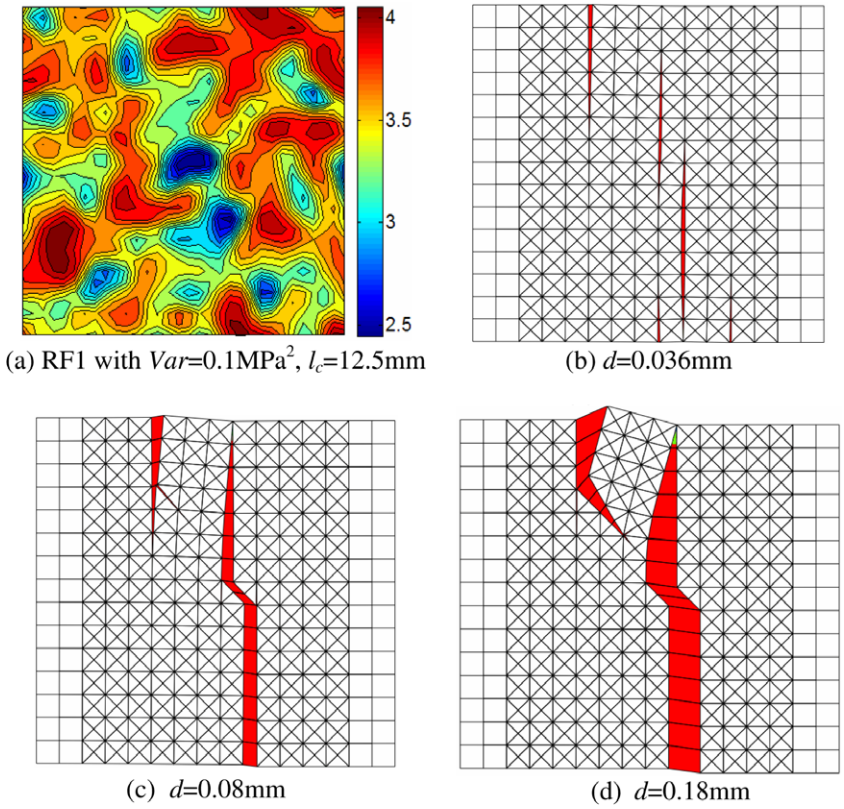

Fig. 6. Fracture process predicted using a typical random sample RF1.

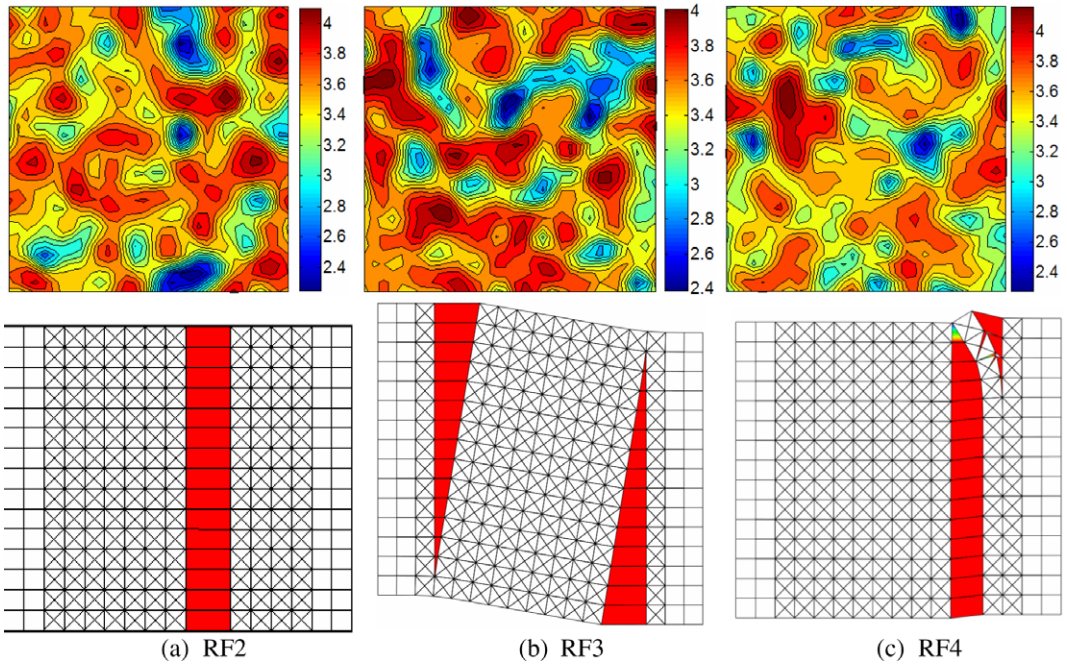

Fig. 7. Simulated crack patterns for typical random samples using the coarse mesh.

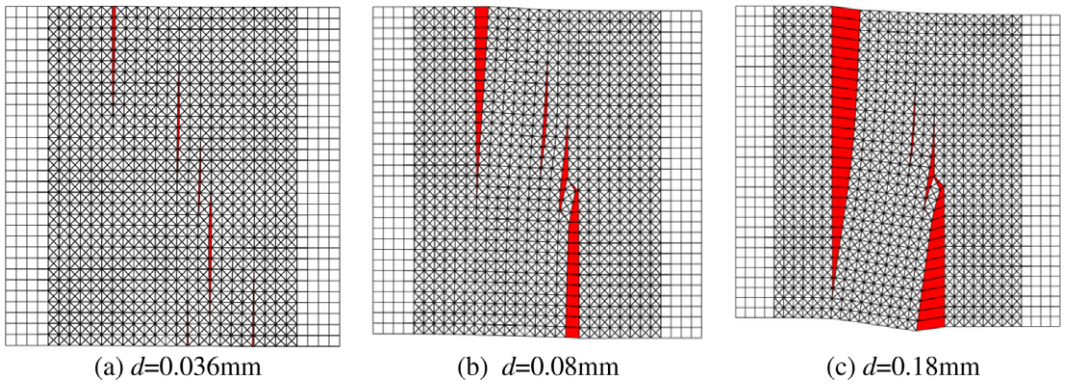

Fig. 8. Fracture process predicted using RF1 (Fig. 6a) and the fine mesh.

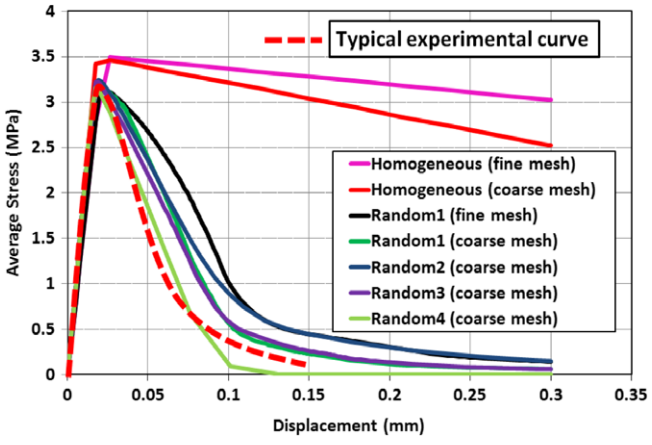

Fig. 9. Comparison of average stress–displacement curves.

fraction $DEF = 2 \times 10^{-4}$ (artificial damping). The default automatic load incrementing with Newton–Raphson method was used. The CPU time taken to reach $d = 0.3$ mm varied considerably, depending on the random fields used. For example, it was 156, 52, 116 and 90 s, respectively, for RF1, RF2, RF3 and RF4 when the coarse mesh was used. This is a reflection of random heterogeneity of the tensile strength, i.e., cracks propagate and merge more easily so that the equilibrium is reached faster in some cases than in others. When the fine mesh was used, the CPU time was typically 5 times more, e.g., 890 s when RF1 was used.

The Monte Carlo simulation with 500 random samples ($Var = 0.1$ MPa^2 and $l_c = 12.5$ mm) was then conducted for the coarse mesh. It was found that all analyses successfully passed the peak point in the load–displacement curves, but nearly one third failed by divergence due to localised stability well before $d = 0.3$ mm was reached. This numerical instability due to material softening often happens in nonlinear fracture problems, when classical Newton–Raphson method is used (Yang and Proverbs, 2004). A few measures were tried to tackle the instability problem: (i) using the modified Riks method which is designed in Abaqus specially to solve unstable problems with material softening or buckling; (ii) limiting the maximum allowable loading increment Δd; (iii) specifying higher *DEF* in the option "Stabilize" to increase the artificial damping; and (iv) using Abaqus/explicit dynamic solver for quasi-static analysis.

The effectiveness of these measures was investigated by modelling a typical random sample using the coarse mesh. The load–dis-

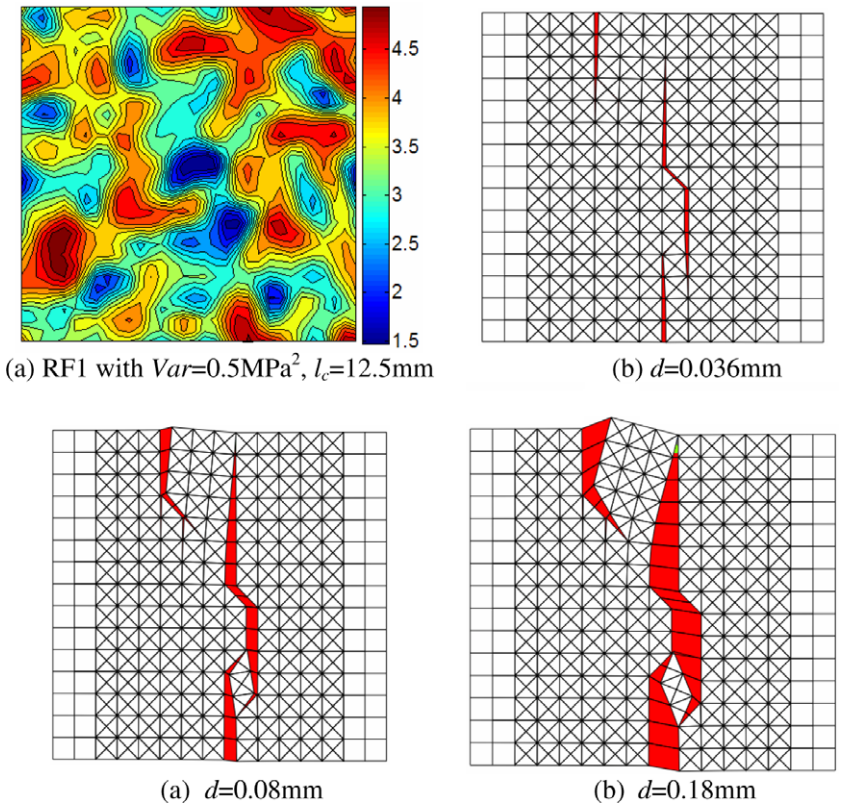

Fig. 10. Fracture process predicted using RF1 and the coarse mesh.

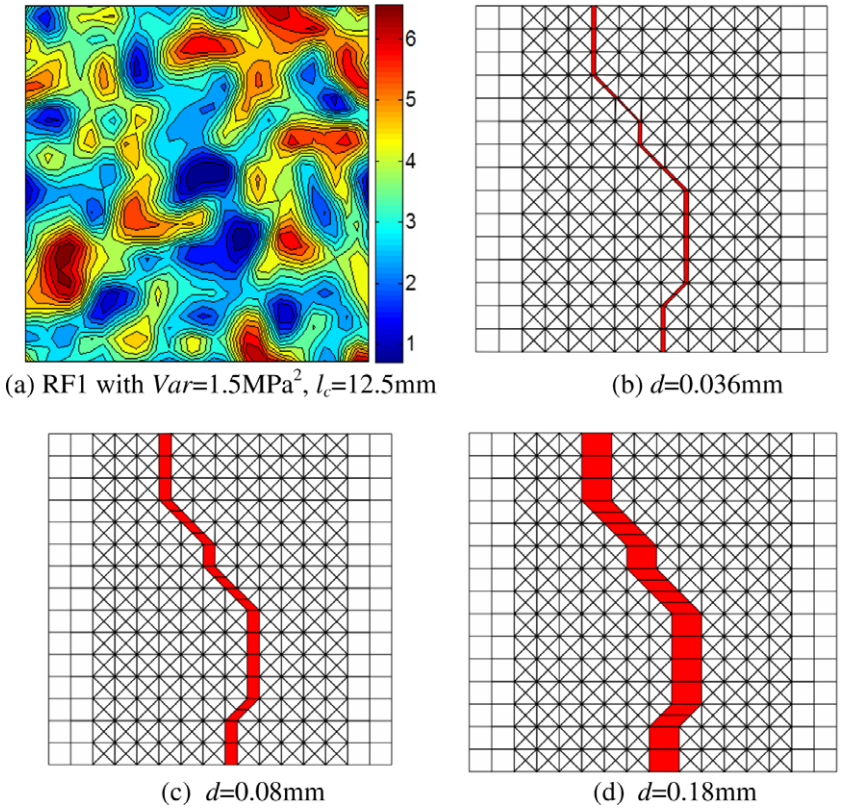

Fig. 11. Fracture process predicted using RF1 and the coarse mesh.

placement curves are compared in Fig. 13. The standard solver failed at $d = 0.05$ mm. The modified Riks method did not lead to any improvement. By limiting the maximum increment to $\Delta d = 0.3 \times 10^{-4}$ mm, the standard solver managed to reach $d = 0.3$ mm but with a high computing time of over 2 h. This indicates that the standard solver using the default automatic incre-

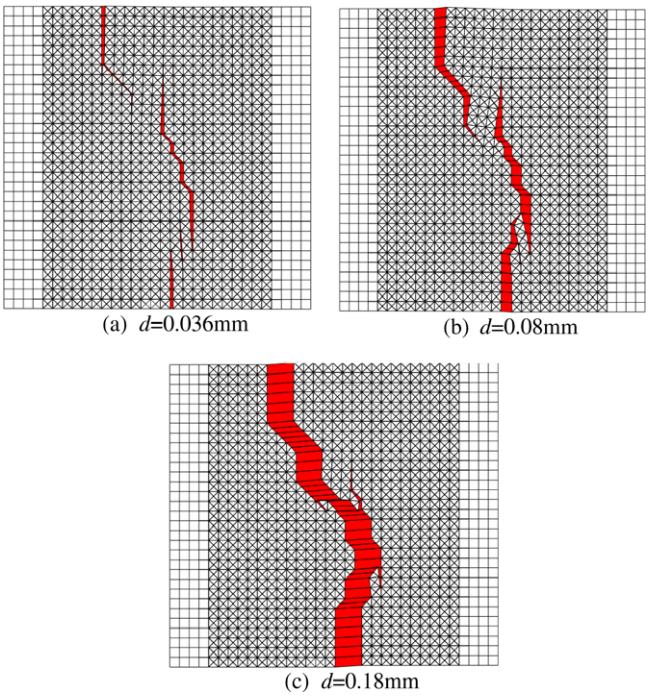

Fig. 12. Fracture process predicted using RF1 and the fine mesh ($Var = 1.5$ MPa^2).

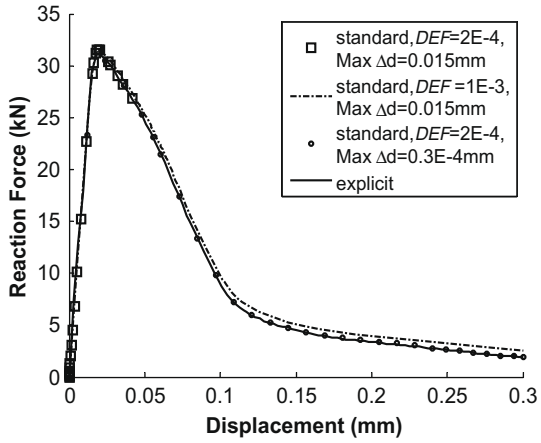

Fig. 13. Load–displacement curves predicted by standard and explicit solvers.

menting is often ineffective in modelling problems with material softening. Increasing the *DEF* to 1×10^{-3} led to a full load–displacement curve but the predicted post-peak branch becomes inaccurate due to excessive artificial damping. The dynamic explicit solver, using a total loading time $t = 0.01$ s, small time increments (typically $\Delta t = 3 \times 10^{-7}$ s) and mass scaling factor *MSF* = 5, was able to predict the full curve accurately with a reasonable 330 s CPU time.

The total loading time t modelled in the Abaqus/explicit solver for quasi-static problems, and the mass scaling factor *MSF* have significant effects on the computational efficiency and accuracy of results. On the one hand, the total loading time t must be long enough to minimise the dynamic effect; on the other, a longer loading time means higher computing cost. Fig. 14 compares the load–displacement curves from a typical random sample and the coarse mesh with different t. It can be seen that $t = 0.01$ and 0.1 s lead to identical curves, but $t = 0.003$ s results in oscillation, a sign of existence of dynamic effect which should be avoided in

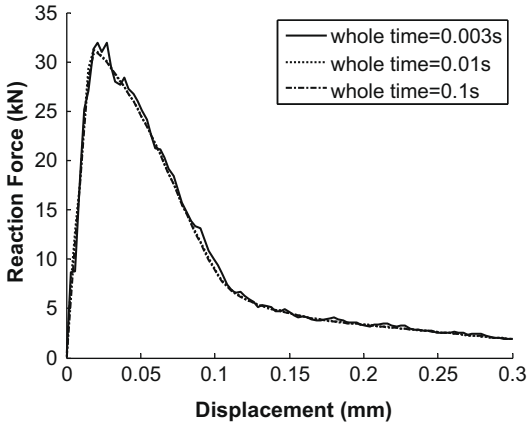

Fig. 14. Load–displacement curves predicted by the explicit solver: effect of loading time ($MSF = 5$).

quasi-static analyses. The CPU times for $t = 0.1$, 0.01 and 0.003 s are 2600, 330 and 150 s, respectively. Fig. 15 shows the results using different mass scaling factors. Similar to the effect of t, a lower *MSF* leads to more accurate results but with longer computing time, and a higher *MSF* produces undesired dynamic effects though with low computing cost. Therefore, compromises must be made between the efficiency and the accuracy when t and *MSF* are selected for quasi-static analyses using Abaqus/explicit.

3.6. Results of Monte Carlo simulations and implications on structural design

Considering the robustness of the Abaqus/explicit solver, it was used in all the following analyses with $t = 0.01$ s and *MSF* = 5. A typical analysis using the coarse mesh takes about 330 s CPU time. The CPU time is also dependent on the number of output frames specified by the user. 200 frames were acquired in each simulation for plotting smooth curves. So an MCS with 500 samples takes about 45 h in total, which is bearable for personal computers. The total time can be significantly reduced by parallel computation, which is now readily available on many computers with multiple CPUs.

Three examples of MCS results are shown in Fig. 16a–c, using the same variance $Var = 0.1$ MPa^2 and three correlation lengths of l_c=6.25, 12.5 and 25 mm, respectively. The mean load–displacement curve, the mean value and the standard deviation of the peak load are also calculated.

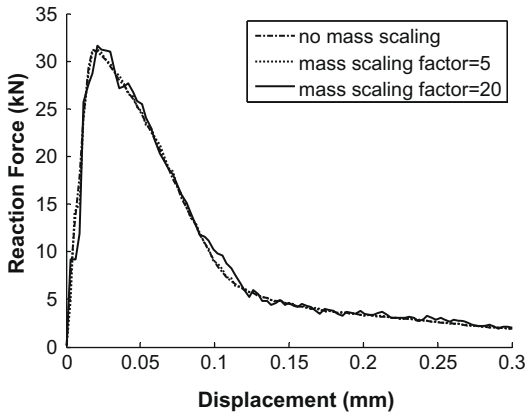

Fig. 15. Load–displacement curves predicted by the explicit solver: effect of mass scaling factor ($t = 0.01$ s).

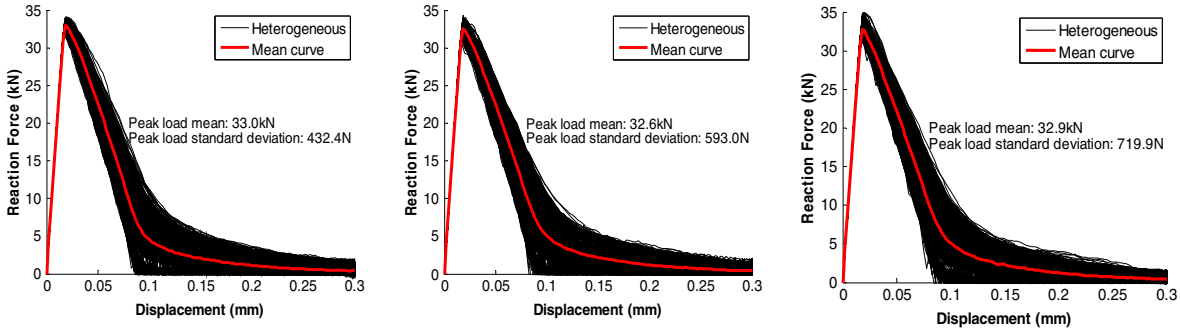

(a) l_c=6.25mm (b) l_c=12.5mm (c) l_c=25mm

Fig. 16. Load–displacement curves predicted from Monte Carlo simulation with 500 samples ($Var = 0.1\ \mathrm{MPa}^2$).

The mean load–displacement curves from all the nine MCS are shown in Fig. 17a–c. It can be seen that for this specimen, the effects of the correlation length on both the peak load and the shape of the mean curve are small for a given variance. The same results are presented in a different way in Fig. 18a–c where the curves in each chart have a constant correlation length. Clearly the variance has a significant effect on the peak load of the mean load–displacement curves. The average peak load from the three variances is 32.8, 29.8 and 26.1 MPa, respectively. For all the correlation lengths investigated, a higher variance results in a lower peak load. As for the predicted crack patterns discussed in Section 3.4, this is because more cohesive elements in larger areas are mobilised to resist fracture when the variance is small, leading to a higher mean peak load. When the variance is large, the "weakest link" or the crack path can be more easily found because fewer weak cohesive elements contribute to fracture resistance, which results in lower mean peak load. This means a higher heterogeneity in the material properties results in structures with lower strength. This may explain to some extent why the fibre-reinforced concrete has higher fracture resistance and strength than plain concrete: fibres make concrete more homogeneous with smaller variance in tensile strength, whereas in plain concrete, the variance is higher due to incompatible strength between aggregate, cement and defects.

Figs. 19–21 show the probability density function (*PDF*) of the peak load for the nine Monte Carlo simulations. The mean, standard deviation and the best-fit Gaussian *PDF* curve $p(x)$ are also shown. It should be noted that although the peak loads from all the MCS appear to closely follow the Gaussian or normal distribution, the exact left tail of the distribution should be Weibullian (Bazant et al., 2007; Vorechovsky, 2007). The Gaussian *PDF* curves are used herein because they are commonly used in structural design. Again, the correlation length has little influence on the mean peak loads whereas a higher variance results in a lower mean peak load (thus a lower structural strength). However, both parameters (especially the tensile strength) affect the standard deviation of the peak load, which is an indicator of structural reliability. For

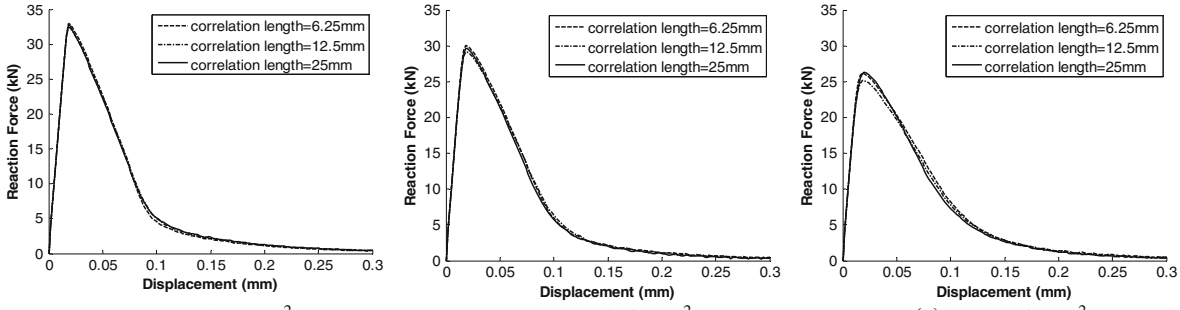

(a) Var=0.1MPa^2 (b) Var=0.5MPa^2 (c) Var =1.5MPa^2

Fig. 17. Mean load–displacement curves: effect of correlation length.

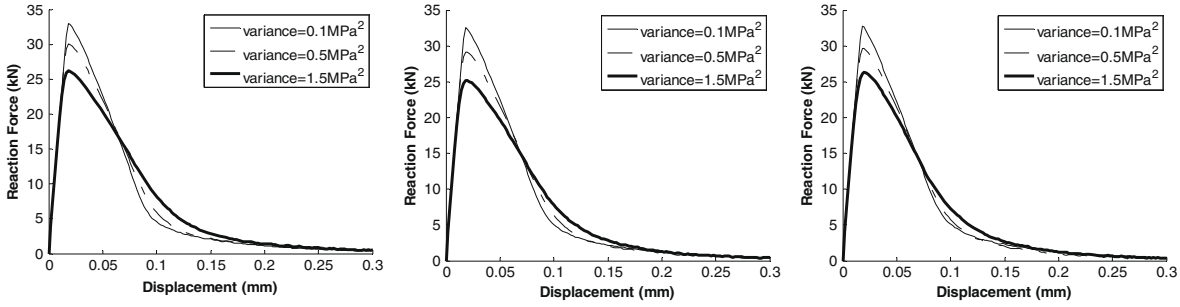

(a) l_c=6.25mm (b) l_c=12.5mm (c) l_c=25mm

Fig. 18. Mean load–displacement curves: effect of variance.

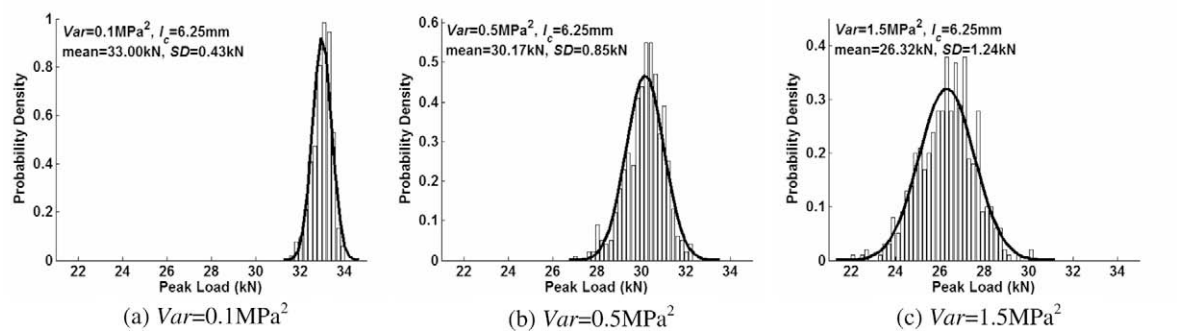

Fig. 19. Probability density of the peak load: $l_c = 6.25$ mm.

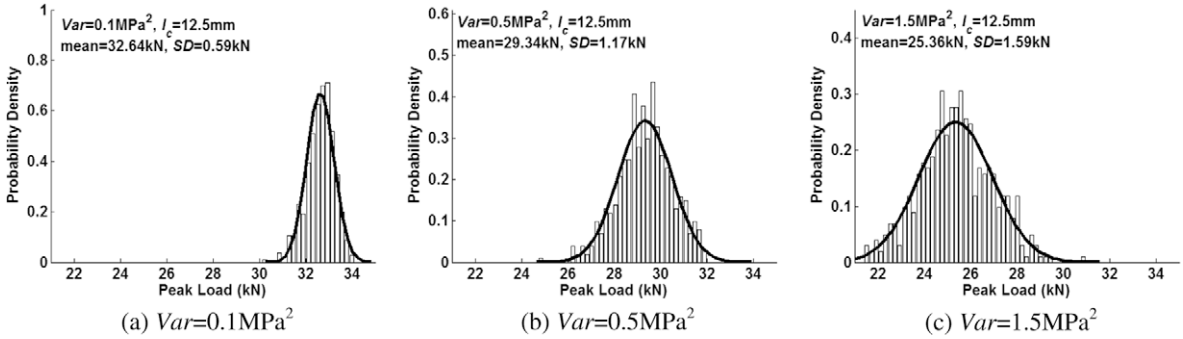

Fig. 20. Probability density of the peak load: $l_c = 12.5$ mm.

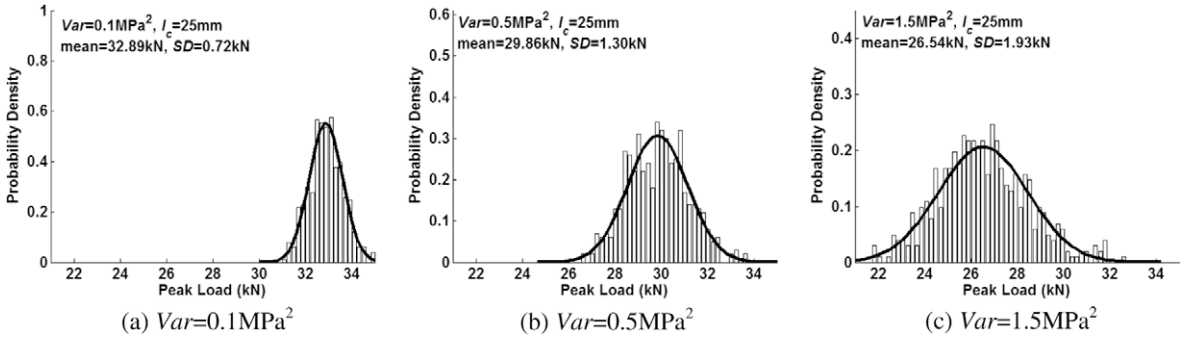

Fig. 21. Probability density of the peak load: $l_c = 25$ mm.

the same correlation length, when the heterogeneity increases due to an increase of the strength variance, the standard deviation of the peak load increases, leading to a less reliable structure. In the extreme case when the strength variance is zero, the material becomes homogeneous and has the highest strength and 100% reliability (zero standard deviation). Of course such purely homogeneous materials do not exist in reality.

The probability density curves $p(x)$ in Figs. 19–21 may be used in reliability analysis of existing structures and design of new structures. For example, assuming the external load F_d is known, the structural reliability can be calculated as

$$P = \int_{F_d}^{\infty} p(x)dx \tag{12}$$

or the failure probability as (1-P).

In many structural design codes, the design strength of a material is based on the characteristic strength, which is usually obtained from physical experiments. For example, in the concrete structures design code Eurocode (BSI, 2001) the characteristic strength of concrete f_k is calculated as,

$$f_k = f_m - 1.64 * SD \tag{13}$$

where f_m is the mean strength and the coefficient 1.64 ensures a 95% confidence in a Gaussian distribution.

Table 1 summarises the mean and the standard deviation of the peak load, the characteristic nominal strength and the failure probability against $F_d = 27$kN as an example for the nine MCS conducted. Provided that the underlying Weibull random fields accurately describe the material heterogeneity (this can only be achieved by detailed statistical analyses of a large number of sophisticated physical experiments), the numerical method developed here may be able to characterise material strength and predict the reliability of existing structures.

3.7. Effect of the number of samples in Monte Carlo simulations

For each MCS in this study, 500 samples of random fields were generated and analysed to ensure that the results were statistically converged. The number of samples required, however, may vary with the values of the parameters. Fig. 22a–c show the relationship

Table 1
Statistics of Monte Carlo simulation results.

Correlation length (mm)	Variance (MPa^2)	Mean of peak load (kN)		Standard deviation of peak load (kN)		Failure probability against a design load of 27 kN		Characteristic nominal strength (MPa)	
			Average		Average	%	Average (%)		Average
6.25	0.1	33.00	29.83	0.43	0.84	0	23.6	3.23	2.85
	0.5	30.17		0.85		0.01		2.88	
	1.5	26.32		1.24		70.83		2.43	
12.5	0.1	32.64	29.11	0.59	1.12	0	29.1	3.16	2.73
	0.5	29.34		1.17		2.28		2.74	
	1.5	25.36		1.59		84.88		2.28	
25	0.1	32.89	29.76	0.72	1.32	0	20.3	3.17	2.76
	0.5	29.86		1.30		1.39		2.78	
	1.5	26.54		1.93		59.42		2.33	

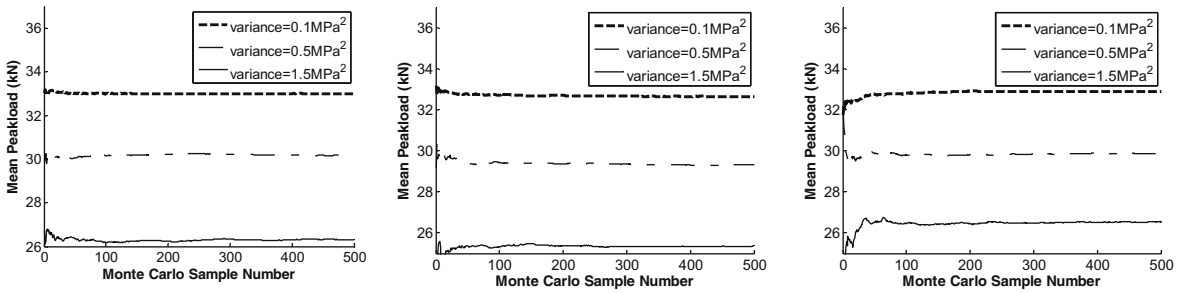

(a) l_c=6.25mm (b) l_c=12.5mm (c) l_c=25mm

Fig. 22. Effect of the number of MCS samples on mean the peak load.

between the mean peak load with the number of samples for the nine MCS. The peak load converges at about 100 samples for all the nine MCS (Fig. 22). In other words, for the peak load to statistically converge, only 100 random samples and nonlinear analyses are required for each of the nine MCS using the coarse mesh. One MCS will then take only 9 h. However, the number of samples required for the *SD* to converge is about 100, 250 and 340, for $l_c = 25$, 12.5 and 6.25 mm, respectively, as shown in Fig. 23. This indicates that the standard deviation converges more slowly than the peak load. It may be noted that the convergence point on a curve is sometimes difficult to identify (dependent on the accuracy required as well), making an objective selection of the number of samples required difficult. An implication for structural design is that, when the characteristic strength of material is evaluated from experiments, a sufficient number of samples should be tested.

4. Conclusions

A computational modelling method has been developed to simulate the complex 2D crack propagation process in quasi-brittle materials with random heterogeneous fracture properties. A concrete specimen under uniaxial tension has been modelled to illustrate the method. The following main conclusions can be drawn:

(1) The homogeneous model assuming uniformly distributed fracture properties throughout the domain of analysis predicts unrealistic crack patterns and incorrect load–displacement curves, which are strongly dependent on the initial mesh. In contrast, the heterogeneous model is capable of predicting realistic complex crack propagation and accurate load-carrying capacity with much improved mesh-objectivity.
(2) The explicit dynamic solver in Abaqus is more robust than the implicit standard solver, which often leads to divergence due to local instability when material softening is experienced.
(3) Extensive Monte Carlo simulations have demonstrated that an increase of the variance in the Weibull random fields of tensile strength with increased heterogeneity leads to a reduction in the mean peak load and an increase in the standard deviation.

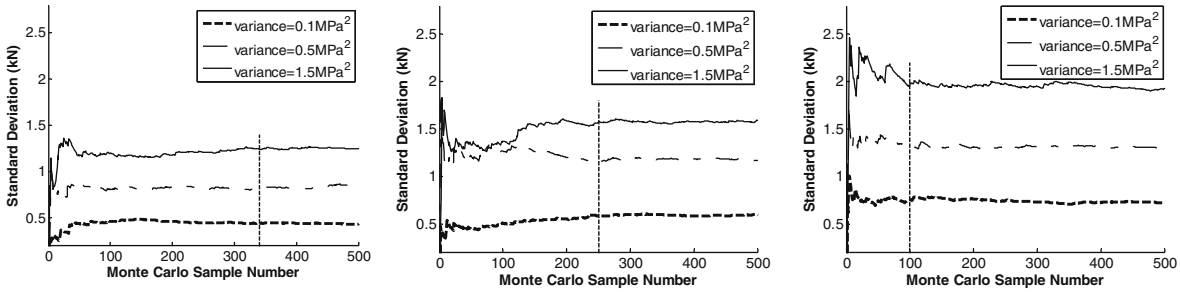

(a) l_c=6.25mm (b) l_c=12.5mm (c) l_c=25mm

Fig. 23. Effect of the number of MCS samples on the standard deviation of the peak load.

(4) The proposed method has the potential of being a simple but effective numerical tool for assessing structural reliability and for calculating the characteristic strength of materials for structural design.

Acknowledgements

This study was supported by EPSRC UK (No.: EP/F00656X/1). X.T. Su's one-year visit to the University of Liverpool was supported by the China Scholarship Council and the National Natural Science Foundation of China (No. 50579081). We thank A/Prof. X.F. Xu at Stevens Institute of Technology USA for providing the computer program used to generate Weibull random fields.

References

ABAQUS 6.7, User documentation, Dessault systems, 2007.
Al-Ostaz, A., Diwakar, A., et al., 2007. Statistical model for characterizing random microstructure of inclusion–matrix composites. Journal of Materials Science 42 (16), 7016–7030.
Altus, E., Givli, S., 2004. Fracture mechanics of a randomly heterogeneous double cantilever beam. International Journal of Fracture 130 (4), 743–763.
Au, S.K., Beck, J.L., 2001. Estimation of small failure probabilities in high dimensions by subset simulation. Probabilistic Engineering Mechanics 16 (4), 263–277.
Barenblatt, G.I., 1959. The formation of equilibrium cracks during brittle fracture: general ideas and hypothesis, axially symmetric cracks. Applied Mathematics and Mechanics 23, 622–636.
Bazant, Z.P., Planas, J., 1998. Fracture and Size Effect in Concrete and Other Quasibrittle Materials. CRC Press, Boca Raton and London.
Bazant, Z.P., Pang, S., Voechovsky, M., Novák, D., 2007. Energetic-statistical size effect simulated by SFEM with stratified sampling and crack band model. International Journal for Numerical Methods in Engineering 71, 1297–1320.
Blair, S.C., Cook, N.G.W., 1998. Analysis of compressive fracture in rock using statistical techniques: Part II. Effect of microscale heterogeneity on macroscopic deformation. International Journal of Rock Mechanics and Mining Sciences 35 (7), 849–861.
Bruggi, M., Casciati, S., et al., 2008. Cohesive crack propagation in a random elastic medium. Probabilistic Engineering Mechanics 23 (1), 23–35.
BSI (2001). BS EN 206-1:2000 Concrete Part I: Specification, Performance, Production and Conformity.
Caballero, A., Lopez, C.M., et al., 2006. 3D meso-structural analysis of concrete specimens under uniaxial tension. Computer Methods in Applied Mechanics and Engineering 195 (52), 7182–7195.
Carmeliet, J., Hens, H., 1994. Probabilistic nonlocal damage model for continua with random-field properties. Journal of Engineering Mechanics 120, 2013–2027.
Carpinteri, A., Cornetti, P., Puzzi, S., 2006. Scaling laws and multiscale approach in the mechanics of heterogeneous and disordered materials. Applied Mechanics Review 59, 283–304.
Cusatis, G., Bazant, Z.P., et al., 2003a. Confinement-shear lattice model for concrete damage in tension and compression: I. Theory. Journal of Engineering Mechanics 129 (12), 1439–1448.
Cusatis, G., Bazant, Z.P., et al., 2003b. Confinement-shear lattice model for concrete damage in tension and compression: II. Computation and validation. Journal of Engineering Mechanics 129 (12), 1449–1458.
Dugdale, D.S., 1960. Yielding of steel sheets containing slits. Journal of Mechanics of Physics and Solids 8, 100–104.
Espinosa, H.D., Zavattieri, P.D., 2003a. A grain level model for the study of failure initiation and evolution in polycrystalline brittle materials. Part I: Theory and numerical implementation. Mechanics of Materials 35 (3-6), 333–364.
Espinosa, H.D., Zavattieri, P.D., 2003b. A grain level model for the study of failure initiation and evolution in polycrystalline brittle materials. Part II: Numerical examples. Mechanics of Materials 35 (3–6), 365–394.
Ganapathysubramanian, B., Zabaras, N., 2007. Modeling diffusion in random heterogeneous media: data-driven models, stochastic collocation and the variational multiscale method. Journal of Computational Physics 226 (1), 326–353.
Graham-Brady, L., Xu, X.F., 2008. Stochastic morphological modeling of random multiphase materials. Journal of Applied Mechanics-Transactions of the ASME 75 (6) (Article No. 061001.).
Gutierrez, M.A., De Borst, R., 1999. Deterministic and stochastic analysis of size effects and damage evolution in quasi-brittle materials. Archive of Applied Mechanics 69 (9-10), 655–676.
Hillerborg, A., Modeer, M., Petersson, P., 1976. Analysis of crack formation and crack growth in concrete by means of fracture mechanics and finite elements. Cement and Concrete Research 6, 773–782.
Hordijk, D.A., 1992. Tensile and tensile fatigue behaviour of concrete; experiments, modeling and analyses. HERON 37, Stevin Laboratory and TNO Research, Delft.
Kassner, M.E., Nemat-Nasser, S., Suo, Z., et al., 2005. New directions in mechanics. Mechanics of Materials 37, 231–259.
Koutsourelakis, P.S., Deodatis, G., 2006. Simulation of multidimensional binary random fields with application to modeling of two-phase random media. Journal of Engineering Mechanics 132 (6), 619–631.
Lopez, C.M., Carol, I., et al., 2008a. Meso-structural study of concrete fracture using interface elements. I: numerical model and tensile behavior. Materials and Structures 41 (3), 583–599.
Lopez, C.M., Carol, I., et al., 2008b. Meso-structural study of concrete fracture using interface elements. II: compression, biaxial and Brazilian test. Materials and Structures 41 (3), 601–620.
Most, T., 2005. Stochastic crack growth simulation in reinforced concrete structures by means of coupled finite element and meshless methods. Ph.D. Thesis, Bauhaus-Universität, Weimar.
Oden, J.T., Belytschko, T., Babuska, V., Hughes, T.J.R., 2003. Research directions in computational mechanics. Computer Methods in Applied Mechanics and Engineering 192, 913–922.
Papadrakakis, M., Papadopoulos, V., Lagaros, N.D., Oliver, J., Huespe, A.E., Sanchez, P., 2008. Vulnerability analysis of large concrete dams using the continuum strong discontinuity approach and neural networks. Structural Safety 30, 217–235.
Pearce, C.J., Kaczmarczyk, L. 2008. Multi-scale multi-grid finite element analysis of concrete. In: Ninth International Conference on Computational Structures Technology, 2008, Saxe-Coburg Publications, Athens.
Sfantos, G.K., Aliabadi, M.H., 2007. A boundary cohesive grain element formulation for modelling intergranular microfracture in polycrystalline brittle materials. International Journal for Numerical Methods in Engineering 69 (8), 1590–1626.
Teng, J.G., Zhu, W.C., Tang, C.A., 2004. Mesomechanical model for concrete. Part II: applications. Magazine of Concrete Research 56 (6), 331–345.
Tomar, V., Zhou, M., 2005. Deterministic and stochastic analyses of fracture processes in a brittle microstructure system. Engineering Fracture Mechanics 72, 1920–1941.
Trias, D., Costa, J., et al., 2006. A two-scale method for matrix cracking probability in fibre-reinforced composites based on a statistical representative volume element. Composites Science and Technology 66 (11–12), 1766–1777.
van Mier, J.G.M., 1996. Fracture Processes of Concrete: Assessment of Material Parameters for Fracture Models, CRC Press. ISBN: 0849391237.
Vorechovsky, M., 2007. Interplay of size effects in concrete specimens under tension studied via computational stochastic fracture mechanics. International Journal of Solids and Structures 44, 2713–2715.
Vorechovsky, M., Sadílek, V., 2008. Computational modeling of size effects in concrete specimens under uniaxial tension. International Journal of Fracture 154 (1–2), 27–49.
Webster, C.G., 2007. Sparse grid stochastic collocation techniques for the numerical solution of partial differential equations with random input data. Ph.D. Thesis, Florida State University.
Xu, X.F., 2005. Morphological and multiscale modeling of stochastic complex materials. Ph.D. Thesis, The Johns Hopkins University.
Xu, X.F., Graham-Brady, L., 2005. A stochastic computational method for evaluation of global and local behavior of random elastic media. Computer Methods in Applied Mechanics and Engineering 194 (42–44), 4362–4385.
Yang, Z.J., Proverbs, D., 2004. A comparative study of numerical solutions to nonlinear discrete crack modelling of concrete beams involving sharp snap-back. Engineering Fracture Mechanics 71, 81–105.
Yang, Z.J., Xu, X.F., 2008. A heterogeneous cohesive model for quasi-brittle materials considering spatially varying random fracture properties. Computer Methods in Applied Mechanics and Engineering 197 (45–48), 4027–4039.
Zhou, F.H., Molinari, J.F., 2004. Stochastic fracture of ceramics under dynamic tensile loading. International Journal of Solids and Structures 41, 6573–6596.
Zhu, W.C., Teng, J.G., Tang, C.A., 2004. Mesomechanical model for concrete. Part I: model development. Magazine of Concrete Research 56 (6), 313–330.